AMSI SUMMER RESEARCH SCHOLARSHIPS 2023–24

SET YOUR SIGHTS ON RESEARCH THIS SUMMER

# Topology and Complexity of Braided Magnetic Fields of the Sun

Zachariah Jones

Supervised by Prof. David Pontin

University of Newcastle

AMSI AUSTRALIAN MATHEMATICAL SCIENCES INSTITUTE

**Abstract**

The sun is an incredibly dynamic system that still holds many mysteries still yet to be fully understood by physicists. One of these mysteries at the focus of this report is the Coronal Heating Problem which posits the question as to how, and why is the corona of the sun thousands of degrees hotter than the surface? The partial answer proposed by Parker is the process of magnetic field braiding. We present a summary of concepts of braid and topological entropy that quantitatively measure how 'chaotic' a braid or flow is and how this applies to measuring the energy transported into the solar corona. Additionally we investigate 3 common methods of measuring the topological entropy of 2D flows. These methods are finite-time braiding exponent **(FTBE)**, Line-Segment Growth, Ensemble Topological Entropy Calculation **(E-tec)**. We find that for solar magnetogram feature tracking, **E-tec** is the most promising technique given better estimates with shorter trajectory time, and fewer total trajectories.

## 1 Introduction

The sun is an incredibly dynamic system that is rich with beautiful physics and many mysteries yet to be fully understood. One such problem at the heart of this report is the coronal heating problem. The coronal heating problem is that the solar corona ($\sim 1,000,000$K) is approximatly thousands of degrees hotter than the surface of the sun, with the surface ($\sim 5,000$K)[7]. This unexpected spike in temperature is not yet fully explainable through known processes. However, one leading theory is that the energy is being transported by a process known as magnetic field braiding [6]. This solution first proposed by Parker [5] states the energy transported to the corona originates in the complex and dynamic motions of the solar photosphere driven by convection currents.

Since there is a relationship between the complexity of the underpinning flow and the amount of magnetic field braiding occurring, having an understanding of how to measure this complexity and the differences and similarities of the methods in measuring this is important. This work aims to provide an overview of the different measures of complexity for braids and 2D fluid flows through a quantity called topological entropy and to determine which estimation method would be best applied to photosphere magnetogram trajectory data in future solar magnetic field braiding investigations.

## 2 Topological Entropy

In the investigation of a physical flow a natural question to investigate is the complexity of the flow or in other words, how 'chaotic' a flow is. A quantity developed by Adler et al is called the '*Topological Entropy*'. We will now present the basic definitions of topological entropy.

**Definition 1 (Newhouse and Pignataro [4])**
Let $f : X \to X$ be a continuous self-map of a metric-space X with distance function $d$. Let $\epsilon > 0$, and $n \in \mathbb{Z}^+$. An n-orbit is a sequence, $f(x), f^2(x), ..., f^{n-1}(x)$ of $f$-iterates of a point $x \in X$. Two n-orbits $f^i(x), f^i(y)$ for $0 \le i < n$ are $\epsilon$-distinguishable if there exists a $j \in [0, n)$ where $d(f^j(x), f^j(y)) > \epsilon$. Let $r(n, \epsilon, f)$ be the *maximal* number of $\epsilon$-distinguishable $n$-orbits. Further, let $r(\epsilon, f) = \limsup_{n\to\infty} \frac{1}{n} \log(r(n, \epsilon, f))$.

Finally, let $h(f) = \lim_{\epsilon\to 0} r(\epsilon, f)$

where $h$ is our topological entropy. An equivalent intuition on this quantity is that it represents the amount of information lost per iteration of $f$. This is possible to be seen in Figure 1, since points that were initially arbitrarily close after an iteration of $f$ will no longer be associated.

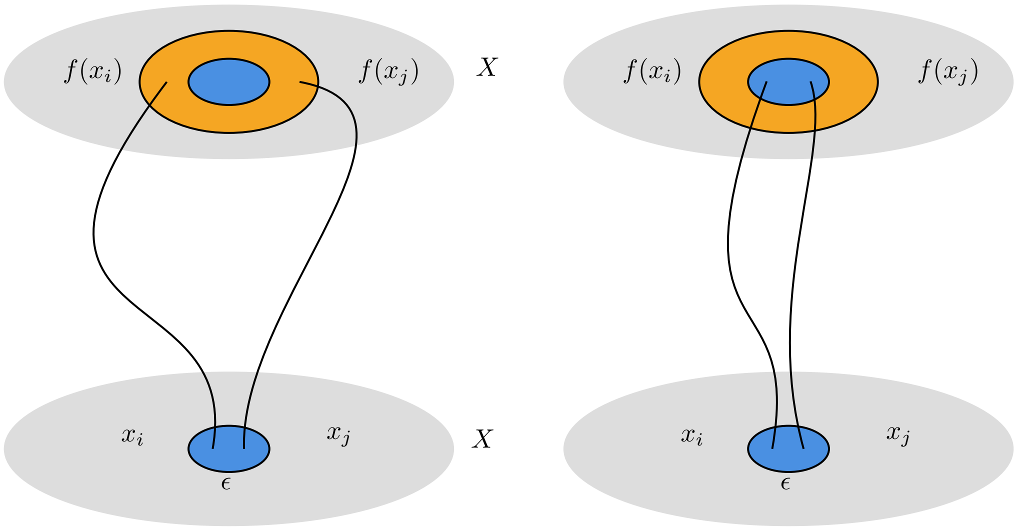


(a) $\epsilon$-distinguishable trajectories (b) non-$\epsilon$-distinguishable trajectories

Figure 1: A diagrammatic representation of what it means for two trajectories in $X$ to be $\epsilon$-distinguishable.

# 3 Braid Entropy

The overall goal of this section is to obtain a lower-bound on the topological entropy of a flow by investigating the topological entropy of braids. To achieve this we will first introduce the braid group and then investigate a bound called the Burau Estimation.

## 3.1 Braid Group

When we refer to the braid group we are really referring to the Artin braid group. We define this groups as:

**Definition 2** The braid group $B_n$ is the group generated by the $n-1$ generators, $\sigma$ that follow the braid relations. $\sigma_i^{+1}$ is the counter-clockwise interchange of the $i^{th}$ strand with the $(i+1)^{th}$ strand seen in Figure 2a. Similarly, $\sigma_i^{-1}$ is a clockwise interchange seen in Figure 2b. The braid relations, as seen in Figure 3 and Figure 4, are given by:

$$\sigma_i \sigma_j = \sigma_j \sigma_i \text{ when } |i-j| > 1$$

$$\sigma_i \sigma_j \sigma_i = \sigma_j \sigma_i \sigma_j \text{ when } |i-j| = 1$$


(a) $\boldsymbol{b} = \sigma_i$ (b) $\boldsymbol{b} = \sigma_i^{-1}$

Figure 2: (a) shows the counter-clockwise rotation of 2 strands in a braid induced by generator $\sigma_i$. (b) shows the clockwise rotation of 2 strands in a braid induced by the generator $\sigma_i^{-1}$.

(a) $\boldsymbol{b} = \sigma_i\sigma_j$ (b) $\boldsymbol{b} = \sigma_j\sigma_i$

Figure 3: Diagram of the $1^{st}$ braid relation $\sigma_i\sigma_j = \sigma_j\sigma_i$ when $|i-j| > 1$

(a) $\boldsymbol{b} = \sigma_i\sigma_j\sigma_i$ (b) $\boldsymbol{b} = \sigma_j\sigma_i\sigma_j$

Figure 4: Diagram of the $2^{nd}$ braid relation $\sigma_i\sigma_j\sigma_i = \sigma_j\sigma_i\sigma_j$ when $|i-j| = 1$

### 3.2 Burau Estimation

**Definition 3** The Burau Representation of a braid is a map from $B_n \mapsto GL\left(\mathbb{Z}\left[t, t^{-1}\right]\right)$
Where, $\sigma_i \mapsto \mathcal{I}_{i-1} \oplus \begin{bmatrix} 1-t & t \\ 1 & 0 \end{bmatrix} \oplus \mathcal{I}_{n-i-1}$
Where $\mathcal{I}_n$ is an $n \times n$ identity matrix and the operation $\oplus$ is the direct sum of matrices.

However there also exists another map, $B_n \mapsto GL_{n-1}\left(\mathbb{Z}\left[t, t^{-1}\right]\right)$, called the *reduced* Burau representation. This can be obtained through a change of basis from the unreduced representation. We will use Thiffeault's definition and interpretation [9].

**Definition 4** The reduced Burau Representation of the braid group, $B_n$, is a map $B_n \mapsto GL_{n-1}\left(\mathbb{Z}\left[t, t^{-1}\right]\right)$, Where, $\sigma_i \mapsto \mathcal{I}_{i-2} \oplus \begin{bmatrix} 1 & t & 0 \\ 0 & -t & 0 \\ 0 & 1 & 1 \end{bmatrix} \oplus \mathcal{I}_{n-i-2}$ and interpret the cases $i = 1$ and $i = n-1$ separately as a deletion of the 1st and last column and row of the respective block.

**Example 1 (The Braid Group on 3 Strands, $B_3$)** For the braid group, $B_3$, there are 4 possible operations: $\sigma_1$, $\sigma_2$, and their respective inverses, $\sigma_1^{-1}$, and $\sigma_2^{-1}$.
For $\sigma_1$, we construct the matrix:

$$\sigma_1 \mapsto \mathcal{I}_{-1} \oplus \begin{bmatrix} 1 & t & 0 \\ 0 & -t & 0 \\ 0 & 1 & 1 \end{bmatrix} \oplus \mathcal{I}_0$$

and so after deletion, we get,

$$\sigma_1 \mapsto \begin{bmatrix} -t & 0 \\ 1 & 1 \end{bmatrix}$$

Similarly for $\sigma_2$, whereby after the deletion of the last row and column, we get,

$$\sigma_2 \mapsto \begin{bmatrix} 1 & t \\ 0 & -t \end{bmatrix}$$

A natural question that arises is whether this representation of the braid groups are faithful. That is to say there does not exist a non-trivial element in the kernel of this map? It has been shown that the representation is unfaithful for $n \geq 5$, and faithful for $n \leq 3$. The $n = 4$ case is still an open problem. Now that we can construct the reduced Burau representation, we now introduce the quantity that provides a lower-bound on the topological entropy.

**Theorem 1** *Given a braid $\beta \in B_n$, the topological entropy of the braid, $h_{braid}$, is bounded by:*

$$h_{braid} \geq \ln \sup_{|t|=1} \left(SR\left(\hat{\beta}\right)\right)$$

*Where, $\hat{\beta}$ is the reduced Burau representation of $\beta$, and $SR$, is the spectral radius of a matrix, defined as the eigenvalue of greatest magnitude.*

An interesting result on this bound is that it is exact for $B_3$ [9]. When equality holds, the estimation is called 'sharp' which can be seen in Figure 6. Of particular interest is the braid, $\beta = \sigma_1\sigma_2^{-1}$. When $n > 3$, the sharpness is not guaranteed and more advanced computational techniques are required such as train-tracks or the computation technique from Moussafir, 2006 [3].

**Example 2 (The Golden/Pigtail Braid)**

The braid at the focus of this investigation is commonly referred to as the golden braid or the pigtail braid. This braid is characterised by the alternating action of a counter-clockwise movement and then a clockwise movement on 3 strands as seen in Figure 5. This is translated into the braid group $B_3$ through the generators $\sigma_1$ and $\sigma_2^{-1}$.

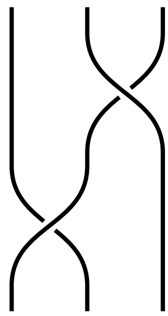

Figure 5: The Golden/Pigtail Braid $\beta = \sigma_1\sigma_2^{-1}$

Let $\beta = \sigma_1\sigma_2^{-1}$, then in the reduced Burau representation we have,

$$\hat{\beta} = \begin{bmatrix} -t & 0 \\ 1 & 1 \end{bmatrix} \begin{bmatrix} 1 & t \\ 0 & -t \end{bmatrix}^{-1}$$
$$= \begin{bmatrix} -t & -t \\ 1 & 1-t^{-1} \end{bmatrix}$$

In general, to determine the $\sup_{|t|=1}$, we set $t = e^{i\theta}$ and vary $\theta$. This gives

$$\hat{\beta} = \begin{bmatrix} -e^{i\theta} & -e^{i\theta} \\ 1 & 1-e^{-i\theta} \end{bmatrix}$$

However, results from Band and Boyland have shown that for $B_3$, this occurs when $t = -1$ which simplifies above to,

$$\hat{\beta} = \begin{bmatrix} 1 & 1 \\ 1 & 2 \end{bmatrix}$$

Which has characteristic polynomial

$$
\begin{aligned}
&\lambda^2 - 3\lambda + 1 = 0 \\
\implies &\lambda = \frac{3 \pm \sqrt{5}}{2} \\
\implies &SR(\hat{\beta}) = \frac{3 + \sqrt{5}}{2} = \varphi^2 \\
\implies &h_{\text{Braid}} = \ln(\varphi^2) \approx 0.962
\end{aligned}
$$

Where $\varphi$ is the golden ratio! Hence why this braid is referred to as the golden braid. In fact, it is a result from D'Alessandro et al. (1999) that this braid has the maximum entropy per generator.

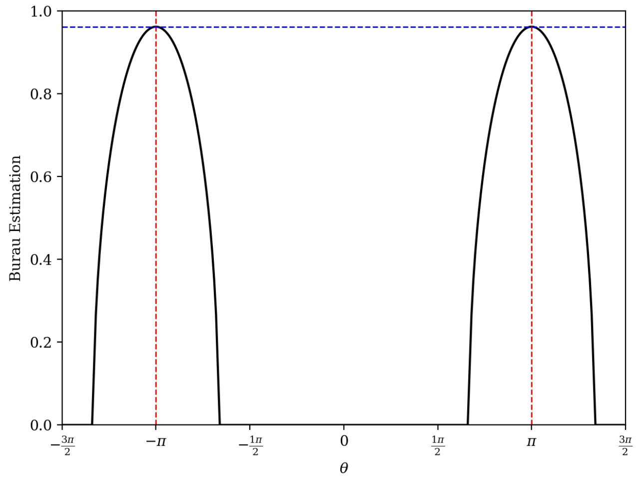


Figure 6: Sharpness of Burau Estimation for $\beta = \sigma_1\sigma_2^{-1}$. The black curve is the $SR\left(\hat{\beta}\right)$, Red lines are located at $\pm\pi$, and the blue line is exact $h_{\text{Braid}}$.

The ability to place a lower-bound on topological entropy will be valuable in determining the nature of future topological estimation methods for the 2D flow that emulates the braiding of magnetic fields on the sun.

# 4 Estimating Topological Entropy

Before we investigate the various methods used to estimate the topological entropy of flows we will introduce the 2D flow that was used to investigate the differences between these methods. We will do this by investigating the methods separately before comparing them all together.

## 4.1 The 2D Flow

The 2D flow we have investigated has previously been used in works to understand the effect of magnetic field braiding on the temperature of the solar corona [2]. It is an Aref blinking flow model given by:

$$\phi_t = \pm x_0 \kappa \sqrt{2\pi} \exp\left[-\frac{(x_t + x_0)^2 + (y_t + y_0)^2}{2}\right] \left(\operatorname{erf}\left(\frac{t - t_c}{2}\right) - \operatorname{erf}\left(\frac{t_0 - t_c}{2}\right)\right)$$

$$x_{t+1} = -(y_t + y_0)\sin(\phi_t) + (x_t \pm x_0)\cos(\phi_t) - x_0$$

$$y_{t+1} = -(x_t \pm x_0)\sin(\phi_t) + (y_t + y_0)\cos(\phi_t) - y_0$$

Where we took $x_0 = 1$, $t_0 = 0$, $t_c = 4 + 8n_{\text{iterations}}$, $y_0 = 0$. $\kappa$ is a free parameter that is a measure of how strongly points are circulated around the center point $\pm x_0$. The parity of $x_0$ is positive if $t \leq 8n_{\text{iterations}}$, else the parity will be negative. This is how we achieve the blinking flow nature. It has been shown that there exists trajectories with periodic orbits of order 3 within this flow for $\kappa = 1$. This allows us to use the lower-bound provided by the braid entropy of $\beta = \sigma_1 \sigma_2^{-1}$ found in Section 4.

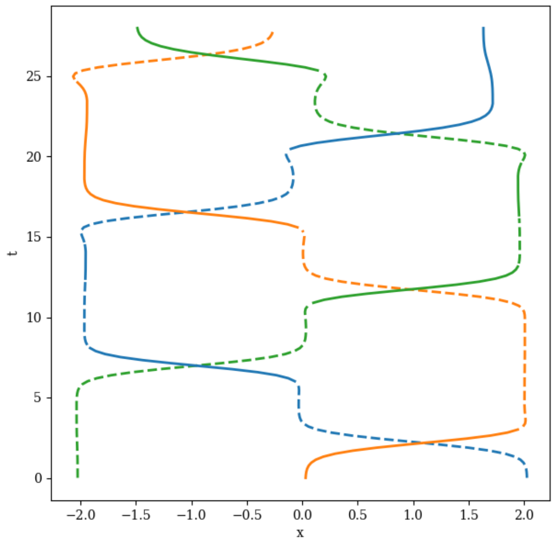


Figure 7: 3 Iterations of the flow above with points $\boldsymbol{p}(x_0, y_0) = (2.025, 0.15)$, $(0.03, -0.29)$, $(-2.025, 0.269)$. Dashed lines are where a trajectory has $y \leq 0.25$, else the lines remain solid. A clear braiding action of $\sigma_2\sigma_1^{-1}$ is occurring within the flow. This braid is conjugate to the golden braid and therefore has the same topological entropy.

### 4.2 Line Segment Growth

A common approach to estimating the topological entropy is by measuring the length dilation of a curve in the flow [2] [4], since the length of a curve is related to the topological entropy.
Let $\gamma$ be a curve and $f$ be the flow.

$$h(f) \geq h(f, \gamma)$$

$$\ell(n_{\text{iterations}}) \approx \ell_0 \exp\left(h(f, \gamma) n_{\text{iterations}}\right)$$

Where $\ell_0$ is the length of $\gamma$ under no iterations of $f$. In this work we have implemented the adaptive algorithm developed by Candeleresi et al. that allows us to directly measure this line segment growth for the line, $y = 0$, $x \in [-2, 2]$. This is done by placing points more specifically where they will be needed (Figure 8). We will now refer to this specific line segment as $\gamma$.
After applying this algorithm while measuring the final length of the line $\gamma$ for varying $\kappa$ we find our topological estimations (Figure 9). For $\kappa = 1$ we find an estimate of $h = 1.14 \pm 0.015$ and for $\kappa = 2.5$ we find $h = 2.49 \pm 0.05$. In fact, fitting a line to the data set we find topological entropy scaling of $h \sim \kappa(0.99 \pm 0.03) + (0.11 \pm 0.04)$. We will find similar linear growth in the alternative methods.

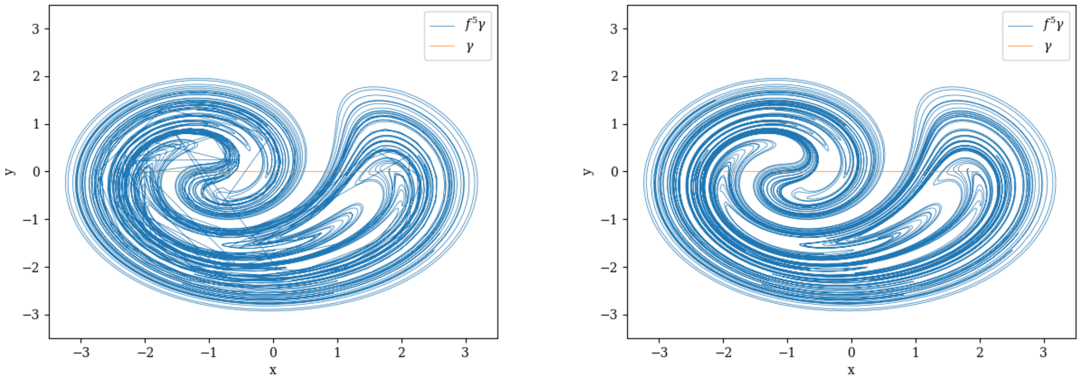


(a) N = 16859 points uniformly distributed

(b) N = 16859 points adaptively distributed

Figure 8: A birds-eye comparison of $\gamma$ after 5 iterations of $f$ without adaptive algorithm and after. Large discontinuities in $f^5\gamma$ without the adaptive algorithm are observed in (a), and after the application of the adaptive algorithm (b), these discontinuities are no longer observed.

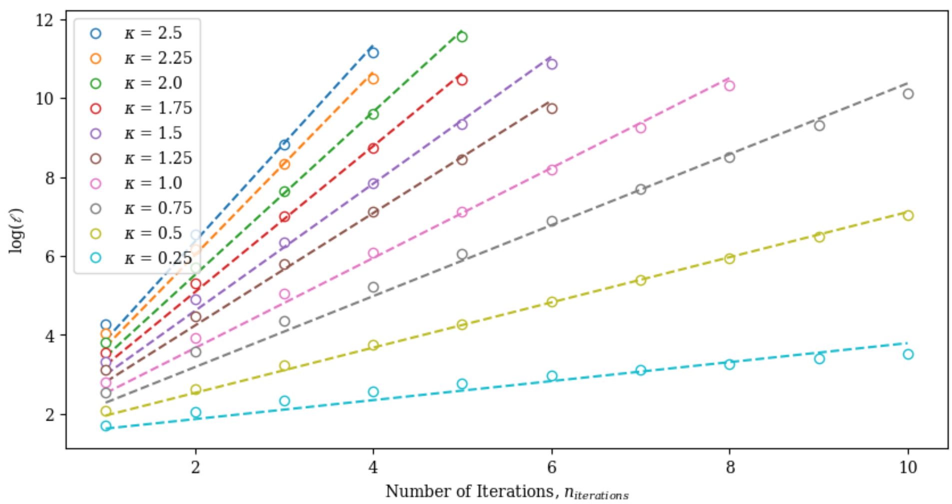


Figure 9: Results from applying adaptive algorithm to directly measure the growth rate of the line segment $\gamma$ for various $\kappa$ with linear fit.

### 4.3 Finite-Time Braiding Exponent

The finite-time braiding exponent (FTBE) estimate developed by Budisic and Thiffeault [1] is a computational method that provides a lower bound on the topological entropy of a system by measuring how $n$ trajectories braid around each other. By fixing a projection angle $\alpha$, one can convert geometric trajectories into a braid $\in B_n$. The quantity being calculated is given in Definition 5 below.

**Definition 5**

Let $\beta$ be a braid corresponding to $n$ strands over a time interval of length, $T$. The finite-time braiding exponent is given by:

$$FTBE(\boldsymbol{b}) = \frac{1}{T}\log\frac{|\beta\ell_E|}{|\ell_E|}$$

Where $\ell_E$ is an initial loop and the length $|\cdot|$ is the number of intersections of the loop with the horizontal axis to the left of a base-point.

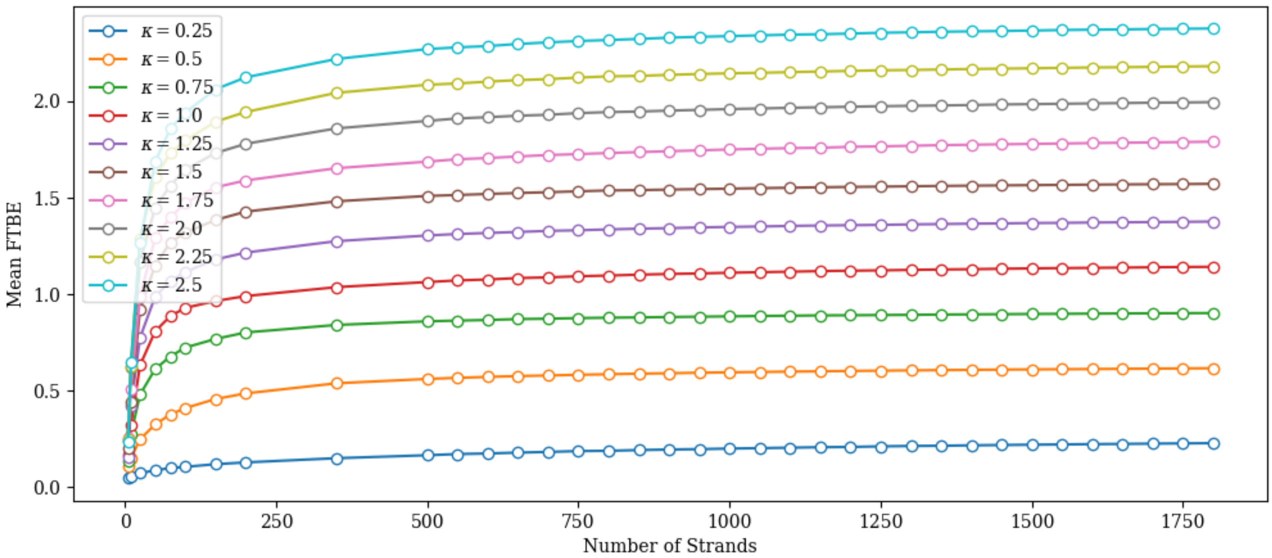


Figure 10: Mean FTBE for varying $\kappa$ showing a convergent nature with increasing the number of strands ($m$) in the sub-braid agreeing with previous studies.

The advantage to FTBE is the fact that it does not require full knowledge of the underpinning flow. All it requires is the relative motion between trajectories and a projection angle. All FTBE calculations were computed within the MATLAB `braidlabs` add-on. From a total $N = 2000$ trajectories of 60 iterations of $\sigma_1\sigma_2^{-1}$ at a projection angle of $\alpha = 0$, we calculated the mean FTBE of 10 uniformly randomly sampled $m$ trajectories where $m < n$.

The convergent nature of the FTBE is still not completely understood. However, with this flow, the convergence does appear to be observed (Figure 10). Since we do not understand the nature of the convergence we cannot make any extrapolations in the limit of infinite strands. Thus, the estimate provided by the FTBE is taken to be the final estimate at $m = 1800$.

### 4.4 Ensemble Topological Entropy Calculation

Similar to FTBE, only requiring relative trajectory movements, a recent method developed by Roberts et al. is the Ensemble-based Topological Entropy Calculation (E-tec) [8]. It tracks the exponential growth of a 'rubber band' through triangulation. The growth rate of the rubber band provides a lower bound on the topological entropy. We calculated the topological entropy of $n = 2000$ trajectories over 60 iterations of $\sigma_1\sigma_2^{-1}$.

### 4.5 Comparison of Techniques

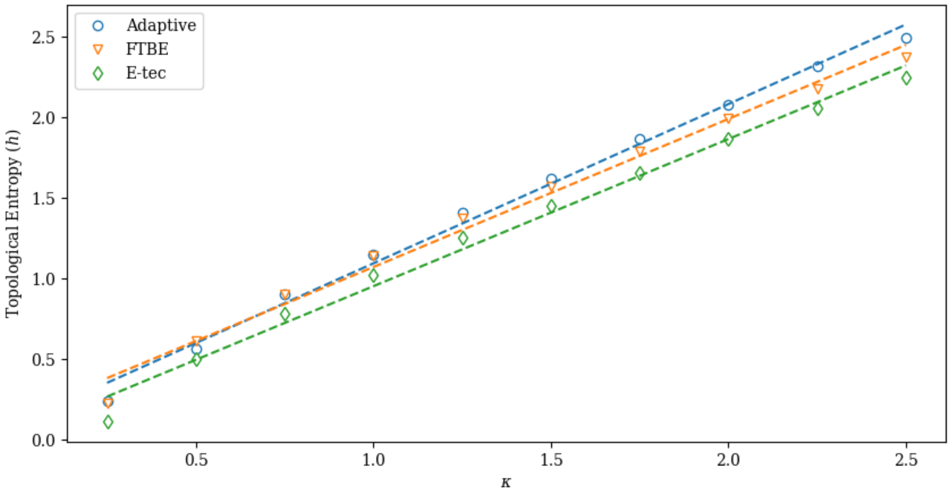


Figure 11: All three methods, Adaptive line segment growth (blue), FTBE (orange), and E-tec (green) showing linear increase in topological entropy estimate.

Comparing the three methods we have computed we find a fairly consistent linear increase in topological entropy with increasing $\kappa$ across all techniques. We find that the adaptive line segment growth technique gives a linear scaling of topological entropy, $h \sim \kappa(0.99 \pm 0.03) + (0.11 \pm 0.04)$, FTBE gives scaling $h \sim \kappa(0.92 \pm 0.03) + (0.15 \pm 0.05)$, and E-tec gives scaling $h \sim \kappa(0.91 \pm 0.03) + (0.04 \pm 0.05)$. Between all three estimation techniques, we are inclined to believe that the adaptive method provides the closest estimation to the true topological entropy since by nature it samples many more points. This is corroborated by its consistently greater value (Figure 11). Focusing on $\kappa = 1$, where it has been shown to have a 3-period orbit, we observe that all three estimates achieve values greater than the lower bound established to be $\log\left(\varphi^2\right) \approx 0.962$ (Figure 12).

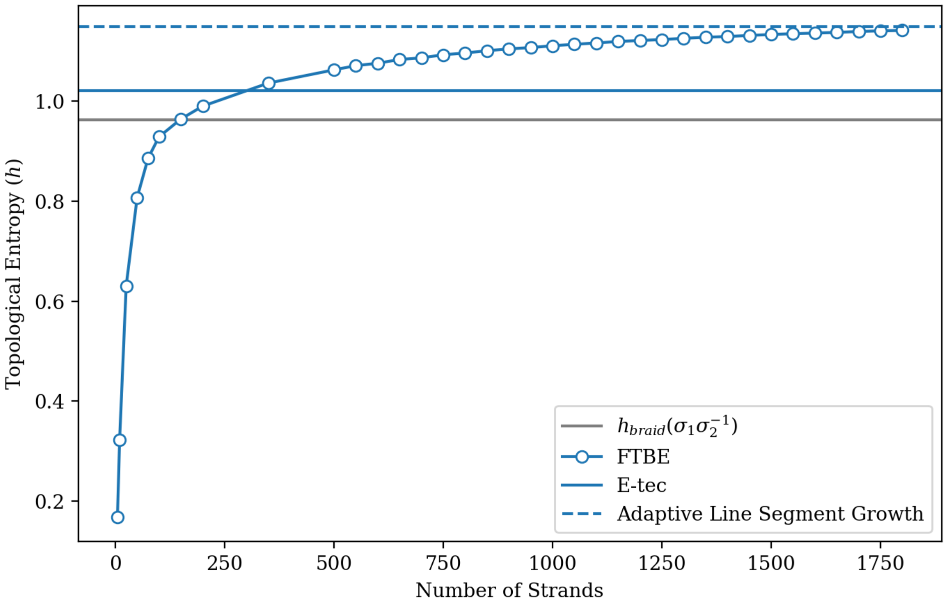


Figure 12: Comparison between adaptive line segment growth (dashed), FTBE (circle), E-tec (blue-solid), and braid entropy lower bound (grey-solid) of $\log\left(\varphi^2\right) \approx 0.962$.

## 5 Conclusion

We have investigated three different estimation techniques for finding the topological entropy of a 2D Aref Blinking Flow. We find that although all three provide consistently similar and great estimations of the true topological entropy, the adaptive line segment growth provided the best estimate in terms of accuracy. Although E-tec provides consistently lower topological entropy estimations, its ability to provide estimations without the need for long observation time, and number of trajectories, we conclude that E-tec is the best candidate for future studies requiring an estimation of topological entropy without full knowledge of the underlying flow.

## References

[1] Marko Budišić and Jean-Luc Thiffeault. "Finite-time braiding exponents". en. In: *Chaos: An Interdisciplinary Journal of Nonlinear Science* 25.8 (Aug. 2015), p. 087407. ISSN: 1054-1500, 1089-7682. DOI: 10.1063/1.4927438. URL: https://pubs.aip.org/cha/article/25/8/087407/135279/Finite-time-braiding-exponents (visited on 02/27/2024).

[2] S. Candelaresi, D. I. Pontin, and G. Hornig. "Quantifying the tangling of trajectories using the topological entropy". en. In: *Chaos: An Interdisciplinary Journal of Nonlinear Science* 27.9 (Sept. 2017), p. 093102. ISSN: 1054-1500, 1089-7682. DOI: 10.1063/1.5000812. URL: https://pubs.aip.org/cha/article/27/9/093102/342106/Quantifying-the-tangling-of-trajectories-using-the (visited on 02/27/2024).

[3] Jacques-Olivier Moussafir. *On computing the entropy of braids*. arXiv:math/0603355. June 2006. URL: http://arxiv.org/abs/math/0603355 (visited on 02/27/2024).

[4] Sheldon Newhouse and Thea Pignataro. "On the estimation of topological entropy". en. In: *Journal of Statistical Physics* 72.5-6 (Sept. 1993), pp. 1331–1351. ISSN: 0022-4715, 1572-9613. DOI: 10.1007/BF01048189. URL: http://link.springer.com/10.1007/BF01048189 (visited on 02/27/2024).

[5] E. N. Parker. "Topological Dissipation and the Small-Scale Fields in Turbulent Gases". en. In: *The Astrophysical Journal* 174 (June 1972), p. 499. ISSN: 0004-637X, 1538-4357. DOI: 10.1086/151512. URL: http://adsabs.harvard.edu/doi/10.1086/151512 (visited on 02/27/2024).

[6] D I Pontin et al. "Braided magnetic fields: equilibria, relaxation and heating". In: *Plasma Physics and Controlled Fusion* 58.5 (May 2016), p. 054008. ISSN: 0741-3335, 1361-6587. DOI: 10.1088/0741-3335/58/5/054008. URL: https://iopscience.iop.org/article/10.1088/0741-3335/58/5/054008 (visited on 02/27/2024).

[7] D.I. Pontin, A.L. Wilmot-Smith, and G. Hornig. "On the Relaxation of Braided Magnetic Fields". en. In: *Procedia IUTAM* 9 (2013), pp. 110–120. ISSN: 22109838. DOI: 10.1016/j.piutam.2013.09.010. URL: https://linkinghub.elsevier.com/retrieve/pii/S2210983813001326 (visited on 02/27/2024).

[8] Eric Roberts et al. "Ensemble-based topological entropy calculation (E-tec)". en. In: *Chaos: An Interdisciplinary Journal of Nonlinear Science* 29.1 (Jan. 2019), p. 013124. ISSN: 1054-1500, 1089-7682. DOI: 10.1063/1.5045060. URL: https://pubs.aip.org/cha/article/29/1/013124/341691/Ensemble-based-topological-entropy-calculation-E (visited on 02/27/2024).

[9] Jean-Luc Thiffeault. *Braids and Dynamics*. en. Vol. 9. Frontiers in Applied Dynamical Systems: Reviews and Tutorials. Cham: Springer International Publishing, 2022. ISBN: 978-3-031-04789-3 978-3-031-04790-9. DOI: 10.1007/978-3-031-04790-9. URL: https://link.springer.com/10.1007/978-3-031-04790-9 (visited on 02/27/2024).